

Prehydration of calcium sulfoaluminate (CSA) clinker at different relative humidities

Lv, Leyang; Šavija, Branko; Li, Lin; Cui, Hongzhi; Han, Ningxu; Xing, Feng

DOI

[10.1016/j.cemconres.2021.106423](https://doi.org/10.1016/j.cemconres.2021.106423)

Publication date

2021

Document Version

Accepted author manuscript

Published in

Cement and Concrete Research

Citation (APA)

Lv, L., Šavija, B., Li, L., Cui, H., Han, N., & Xing, F. (2021). Prehydration of calcium sulfoaluminate (CSA) clinker at different relative humidities. *Cement and Concrete Research*, 144, 1-14. Article 106423. <https://doi.org/10.1016/j.cemconres.2021.106423>

Important note

To cite this publication, please use the final published version (if applicable). Please check the document version above.

Copyright

Other than for strictly personal use, it is not permitted to download, forward or distribute the text or part of it, without the consent of the author(s) and/or copyright holder(s), unless the work is under an open content license such as Creative Commons.

Takedown policy

Please contact us and provide details if you believe this document breaches copyrights. We will remove access to the work immediately and investigate your claim.

Prehydration of calcium sulfoaluminate (CSA) clinker at different relative humidities

Leyang Lv^{a*}, Branko Šavija^b, Lin Li^c, Hongzhi Cui^a, Ningxu Han^a, Feng Xing^a

^a Guangdong Province Key Laboratory of Durability for Marine Civil Engineering, School of Civil Engineering, Shenzhen University, Shenzhen 518060, China;

^b Micromechanics Laboratory (MICROLAB), Faculty of Civil Engineering and Geosciences, Delft University of Technology, Stevinweg 1, 2628 CN Delft, The Netherlands.

^c Saint-Gobain Research (Shanghai) Co., Ltd., Shanghai 200245, China

* Corresponding authors at: School of Civil Engineering, Shenzhen University, Shenzhen 518060, China. E-mail addresses: l.lv@szu.edu.cn (L. Lv).

Abstract:

The use of CSA cement in practice has been hindered by its unstable performance and short shelf-life caused by the prehydration of CSA clinker. In this study, the effect of ambient humidity on the prehydration rate and process of CSA clinker was investigated. The prehydration degree, ageing progress, and the dynamic change of mineral composition of CSA clinker exposed to five different relative humidities (ranging from 23% to 98%) for up to 180 days were studied. Experiments revealed that the ambient humidity of 60% RH can be considered a threshold value for storage of CSA clinker. Exposure of CSA clinker to RH higher than 60% will not only result in a significant decrease of hydraulic reactivity, but also in agglomeration of the clinker. Although the exposure of CSA clinker to RH lower than 60% has little effect on the hydraulic reactivity, the main hydration peak was found to be slightly delayed with the increase of RH.

Keywords:

CSA cement; prehydration; ye'elimite; Anhydrite; phase assemblage

1. Introduction

The production of ordinary Portland cement (OPC) has increased more than 30-fold since 1950, and almost 4-fold since 1990. Especially in developing countries, such as China, the cement production has grown by a factor of almost 12 since 1990. Consequently, 73 % of global growth in Portland cement production during this period occurred in China [1]. A recent study estimated that the total emissions from the cement industry are responsible for up to 5.6 % of global CO₂ emissions [2]. Clearly, current trends in cement production are not sustainable. Therefore, the cement industry is looking for new options to reduce its CO₂ emissions.

Calcium sulfoaluminate (CSA) cement seems to be a promising and eco-friendly alternative to OPC [3, 4]. CSA cement is mainly based on the mineral substance ye'elimite ($4\text{CaO}\cdot 3\text{Al}_2\text{O}_3\cdot \text{SO}_3$, $\text{C}_4\text{A}_3\text{S}$ in

34 cement notation). The production of ye'elimite releases 66% less CO₂ compared to the production of
35 alite (the dominant phase of OPC [5]), due to the lower consumption of calcium carbonate in production.
36 In addition, the production of CSA cement requires a sintering temperature of only 1250 °C, which is
37 about 200 °C lower than the sintering temperature of OPC. Moreover, the grinding process of CSA
38 consumes less energy compared to OPC as the hardness of CSA clinker is relatively low [6]. The
39 combination of these factors makes CSA cement an ideal option for reducing CO₂ emissions of the
40 cement industry. Recent data shows that CSA cement releases only 0.56 g CO₂ per mL cementing phase
41 during production, while alite releases 1.80 g [5]. Apart from environmental advantages, CSA cement
42 also has technical advantages compared to OPC: it has comparable early and late strength with lower
43 shrinkage [7]. Furthermore, the relatively short setting and hardening time can of CSA cement can, to
44 a large extent, promote construction efficiency. Although lower strength and durability issues due to
45 e.g. carbonation are a big concern hindering CSA application in large-scale construction, in-depth
46 studies that can push the application of CSA cement further are of great value.

47 It has been demonstrated that the exposure to water vapour pressure of a certain intensity will lead to
48 prehydration of cement clinker. Moisture is present in the process of cement production, transportation,
49 and storage. Although improved packaging may help, the prehydration of cement cannot be fully
50 prevented. Silica-based clinker minerals, such as tricalcium silicate (C₃S) and dicalcium silicate (C₂S),
51 start to prehydrate at ambient humidity above 85% and 90% RH, respectively [8]. Some hydration
52 products of OPC, such as ettringite, monosulfate and calcium aluminate hydrate, may also undergo a
53 phase deformation or transformation due to the change of ambient climate [9, 10]. Recent work suggests
54 that prehydration of OPC not only results in a decrease in the hydraulic reactivity and prolongation of
55 the setting time [11], but also causes a reduction in the rate of strength development [12, 13]. Dubina et
56 al. [14] attributed the occurrence of prehydration to the surface adsorption of water vapor on the cement
57 grains, which results in a reduction in surface area and changes in surface charge. Thermodynamic
58 analyses were performed to understand the reason C₃S hydration stops below 80% RH on the basis of
59 the change in water activity [15]. Compared to silica-based clinker minerals, aluminate-based clinker
60 minerals such as ye'elimite (the main constituent of CSA cement) and tricalcium aluminate (C₃A) are
61 more susceptible to moisture. C₃A was found to hydrate at ambient humidity of 60% RH [8]. A recent
62 study [13] shows that the exposure of commercial CSA cement to RH above 60% (ranging from 67%-
63 78%) has negative effects on the hydration and strength development of both CSA and CSA-OPC
64 cement pastes. In fact, fast and unpredictable prehydration of CSA cement resulting from accidental
65 moisture exposure has long been a problem in practical applications, especially in tropical and
66 subtropical coastal regions. Although the negative effect of the exposure of CSA cement to ambient
67 humidity has been explored in lab conditions, a quantitative relation between the prehydration degree
68 and the exposure condition has not been established. There is a lack of in-depth knowledge about the
69 degradation of ye'elimite at various RH and how this is linked to the dynamic change of the mineral

70 phases. In addition, it has been reported that the properties of CSA cement depend largely on the calcium
71 sulfate (CaSO_4) content [5, 16]. By changing the molar ratio of gypsum/ye'elimite, the hydration
72 products, setting time, strength development and volume stability of CSA cement can be controlled [5,
73 17]. However, the influence of calcium sulfate addition on the prehydration of CSA clinker is not clear.

74 The aim of this work is to investigate the influence of relative humidity on the prehydration of ye'elimite.
75 This should allow defining a relationship between the ambient humidity and shelf-life of CSA cement.
76 To this end, phase pure ye'elimite was produced using a stoichiometric mixture of calcium carbonate,
77 aluminium oxides and gypsum. The synthetic ye'elimite, with and without addition of anhydrite
78 (CaSO_4), was exposed to five different RH, ranging from 23 to 98%, for a maximum 180 days. The RH
79 was controlled by the saturated salt solution method in sealed conditions at 23 °C. The hydration degree
80 was determined using thermogravimetric analysis (TGA) by calculating the weight loss of chemically
81 bound water. X-ray diffraction (XRD) coupled with Rietveld method was used to investigate the
82 dynamic changes of mineral composition of ye'elimite exposed to various RH. The morphology and
83 the microstructure of mineral grains were observed by using an environmental scanning electron
84 microscope (ESEM). The hydration kinetics of prehydrated ye'elimite was monitored by means of
85 isothermal calorimetry. In the end, based on the result of hydration heat, the influence of prehydration
86 of ye'elimite on its final hydration products was further analysed with the help of TGA and XRD. The
87 findings reported herein do not only contribute to understanding of CSA cement prehydration, but may
88 also provide guidance to the cement industry for better storage and application of CSA clinker in
89 practice.

90

91 **2. Materials and Methods**

92 2.1 Materials

93 Phase pure calcium sulfoaluminate (ye'elimite) clinker mineral was synthesized from a stoichiometric
94 mixture of calcium carbonate (CaCO_3), aluminum hydroxide ($\text{Al}(\text{OH})_3$) and calcium sulfate dihydrate
95 ($\text{CaSO}_4 \cdot \text{H}_2\text{O}$). Potassium acetate, potassium carbonate, sodium bromide, sodium chloride, potassium
96 chloride and potassium sulphate were used to maintain a constant RH value of 23%, 43%, 60%, 85%
97 and 98%, respectively, at 23 °C. Organic solvents, isopropanol and diethyl ether, were used to stop the
98 process of cement hydration, as recommended by RILEM TC-238 SCM [18]. Anhydrite was obtained
99 by burning calcium sulfate dihydrate at 700 °C for 2h. All chemicals used were analytical grade without
100 further purification.

101 2.2 Sample preparation

102 2.2.1 Preparation of ye'elimite

103 Ye'elimite was prepared using reagent grade materials. According to the molecular formula of $C_4A_3\hat{S}$,
104 the molar ratio of $CaCO_3$, $Al(OH)_3$, $CaSO_4 \cdot 2H_2O$ should be 3:6:1. For synthesizing 100 g of ye'elimite,
105 the stoichiometric amounts of $CaCO_3$, $Al(OH)_3$, $CaSO_4 \cdot 2H_2O$ are 49.20, 76.67, 28.20 g, respectively.
106 However, due to the volatilization of sulfur in the sintering process, the weight calculation based on the
107 molar ratio is **not accurate**. Furthermore, the decomposition of $CaSO_4$ will also result in an excess of
108 CaO . To obtain relatively pure $C_4A_3\hat{S}$, the amount of $CaSO_4 \cdot 2H_2O$ and $CaCO_3$ has to be recalculated.
109 Zhang et al. [19] concluded that the volatile content of $CaSO_4$ accounts for around 7% of the total mass
110 of $C_4A_3\hat{S}$. This means that for producing every 100 g $C_4A_3\hat{S}$, 8.85 g extra of $CaSO_4 \cdot 2H_2O$ and 5.15 g
111 less of $CaCO_3$ has to be added to the mixture. The recalculated masses of raw materials, $CaSO_4 \cdot 2H_2O$,
112 $CaCO_3$, $Al(OH)_3$, are 37.06, 44.05, and 76.7 g, respectively.

113 The raw materials were first homogenized in a ceramic bowl with deionized water using a mechanical
114 stirrer for 2 h and then dried at 105 °C for 24 h. The obtained mixture was compacted by hand using a
115 flat pestle in a corundum crucible. The crucible was then placed in a muffle furnace and then sintered.
116 The mix was heated from 20 °C to 900 °C with a heating rate of 5 °C/min, and kept for 1 h at 900 °C.
117 Afterwards, the mix was heated up to 1250 °C applying a heating rate of 10 °C/min. The mix was
118 sintered in the furnace for 3 h at 1250 °C followed by fast cooling (quenching process) in air at lab
119 temperature. The final product was dry-ground manually in a grinding bowl. The grinding process was
120 performed in a glovebox with nitrogen gas protection. Anhydrite was prepared by burning calcium
121 sulfate dihydrate ($CaSO_4 \cdot 2H_2O$) in a furnace at 700 °C for 2 h. To study the influence of calcium sulfate
122 on the **prehydration** of ye'elimite, besides the pure ye'elimite (**henceforth referred to as PY**) clinker
123 mineral, ye'elimite was finely blended with anhydrite with a ye'elimite to anhydrite ratio of 7:3
124 (**henceforth referred to as 7Y3A**). Both clinker types reached the desired fineness of $D_{90} < 40 \mu m$. Purity
125 of the achieved mineral was identified by X-Ray Diffraction (XRD) coupled with Rietveld refinement
126 method. The achieved composition for the two clinkers was: PY - 97.2% ye'elimite and (hard burnt)
127 2.8% anhydrite; 7Y3A - 67.5% ye'elimite, 32.5% anhydrite.

128

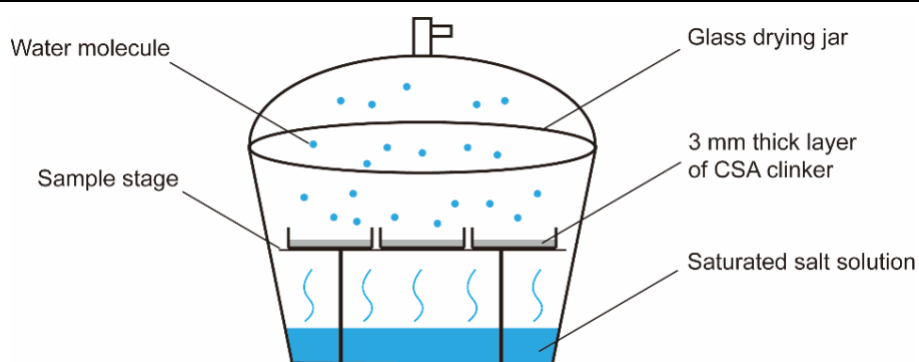
129 2.2.2 Prehydration procedure

130 The clinker minerals were aged at 23%, 43%, 60%, 85% and 98% RH, respectively, for a maximum
131 180 days. The corresponding RHs were maintained in separate sealed glass drying jars using the
132 saturated salt solution method [20]. Ambient temperature, saturated salt solution type, the target RH,
133 and **the standard RH which summarized by National Institute of Standards and Technology (NIST) [21]**
134 are shown in Table 1. To reach equilibrium, the saturated salt solutions were premixed (heated up to
135 90°C followed by cooling down to lab temperature) and left in a glass drying jar for 3 days. Before the
136 exposure of clinker to water vapour, the samples were dried using a silica gel desiccant at the exposure
137 temperature for 1 day. To make sure that the clinker was sufficiently exposed to water vapour, the

138 mineral powder was evenly spread on glass dishes with a layer thickness of 3 mm. The schematic
 139 diagram of the clinker **prehydration** setup is shown in Fig. 1.

140 Table 1. **Prehydration** conditions of PY and 7Y3A clinkers for different exposures.

Environment temperature	Saturated salt solution	Target RH (%)	Standard RH (%)
23 ± 2 °C	Potassium acetate	23	22.51±0.32
	Potassium carbonate	43	43.16±0.39
	Sodium bromide	60	57.57±0.40
	Potassium chloride	85	84.34±0.26
	Potassium sulfate	98	97.3±0.45



141

142 **Fig.1** Schematic diagram of CSA the clinker **prehydration** setup.

143

144 2.2.3 Stoppage of hydration

145 After the samples were aged at different RH for a certain period of time, the aged clinker mineral was
 146 taken out from the glass jar and the hydration was stopped by the solvent exchange method. To do this,
 147 the clinker mineral was immersed in isopropanol and ground in a corundum mill for 15 minutes. The
 148 ground clinker was filtered by vacuum to extract the organic solution. The filtrate was dried in an
 149 aerated oven at 40°C for 10 min and then vacuum sealed in a plastic sample bag. Since long-term storage
 150 could possibly result in an instable mineral composition, analytical measurements such as
 151 **thermogravimetric** analysis (TGA), X-ray diffraction (XRD) and
 152 environmental scanning electron microscopy (ESEM) were performed immediately after stopping the
 153 clinker hydration.

154

155 2.4 Characterization methods

156 The experiments carried out to characterize the **prehydration** process are summarised in Table 2.

157

Table 2. Summary of conducted tests.

Test	Exposure time (Day)
------	---------------------

	0	7	14	28	90	180
Water sorption	√	√	√	√	√	√
TGA	√	√	√	√	√	√
XRD	√	√	√	√	√	√
SEM						√
Calorimetry						√

158

159 The water sorption kinetics of clinker minerals at different RHs was measured by monitoring the
 160 dynamic change of clinker mass. Before the test, the clinker was vacuum dried at 20 °C for 24 hours.
 161 An average of 3 g clinker was weighted, spread evenly on glass sheet, and then stored in the glass jar
 162 with corresponding RH. The water sorption kinetics was reflected by the weight increment ratio (%) of
 163 clinker exposed to water vapour compared to the initial weight of the **dry sample**. To minimize the
 164 experimental error, the samples were weighted immediately as they were taken out from the drying jar.

165

166 The **thermogravimetric** analysis was carried out on each 30 ± 2 mg ground sample using a TGA analyzer
 167 (Q50, TA Instruments, USA) under flowing nitrogen (40 ml/min). The temperature was increased from
 168 30 to 1000 °C at a heating rate of 10°C /min. The degree of hydration, α , was calculated based on the
 169 **thermogravimetric** analysis using the following equation [8, 22]:

$$170 \quad \alpha = \frac{W_{chem.w.}}{W_{max.chem.w.}} - LOI \quad (1)$$

171 All weights in this formula are relative to the ignited clinker weight: g/g ignited clinker. $W_{max.chem.w.}$
 172 is the mass proportion of chemically bound water of the fully hydrated clinker. In this study, the fully
 173 hydrated clinker was defined as PY or 7Y3A clinker hydrated at 23°C for 28 days with a water to cement
 174 ratio of 1. The calculated $W_{max.chem.w.}$ of PY is 0.56 g/g and 7Y3A is 0.65 g/g, respectively. LOI (Loss
 175 On Ignition) is the normalized weight loss of the unhydrated cement, and $W_{chem.w.}$ is the normalized
 176 weight loss of the hydrated sample [23], determined as:

$$177 \quad W_{chem.w.} = \frac{W_{50^{\circ}\text{C}} - W_{550^{\circ}\text{C}}}{W_{550^{\circ}\text{C}}} \quad (2)$$

178 Finally, the physically adsorbed water on the surface of the crystal was calculated by subtracting the
 179 chemically bound water from the overall weight increment after water absorption.

180

181 XRD was performed on the CSA clinker (after stopping the hydration) using a Bruker D8 in a $\theta - 2\theta$
 182 configuration with a monochromatic $\text{CuK}\alpha$ radiation and equipped with the LYNXEYE detector. The
 183 voltage and the current of the generator were set to 40 kV and 40 mA, respectively. The measurement
 184 2θ range was 5° to 70° with a step-size of approximately 0.02°. The quantitative phase assemblages of
 185 the anhydrous and aged clinker, as well as the hydrated paste, were analyzed using the Rietveld method.
 186 Aluminium oxide (Al_2O_3) was applied as an external standard, and was always measured on the same

187 day and under the same measurement conditions as the other samples. The quantitative phase content
188 was recalculated to a anhydrous statue by taking into account the amount of chemically bound water.
189 The mineral phases used in the quantitative phase analysis and their corresponding abbreviations are
190 given in Table 3.

191

192 Table 3 Mineral phases used in the quantitative phase analysis and its corresponding abbreviation.

Mineral phase	Abbreviation	Ref.
Ye'elimite	Y	[24]
Anhydrite	A	[25]
Ettringite	Et	[26]
Monosulfate	Ms	[27]
Gibbsite	AH	[28]
Hannebachite	CS	[29]

193

194 The morphology of clinker mineral particles exposed to various RHs was observed with ESEM (Quanta
195 TM 250 FEG, FEI, United States). To obtain homogeneous dispersion of clinker particles, the clinker
196 powder was first dispersed in isopropanol, and then droplets of the suspension were deposited on a
197 conductive tape glued to a sample holder. Upon complete evaporation of isopropanol, the dried samples
198 were coated with a gold film and subjected to ESEM observations.

199

200 The hydration heat of samples aged at different RHs during the first 48 h was measured with an 8-
201 channel isothermal calorimeter (Thermometric TAM Air). The ambient temperature was set to 23 °C.
202 3.2 g of aged CSA clinker and 3.2 g of deionized water were poured into a glass vial and mixed (outside
203 of the calorimeter) using a laboratory mixer for 30 s to obtain a water/binder ratio of 1. The glass vial
204 was then sealed with a cap and placed into the calorimeter. Since the initial peak was found not to be
205 significantly influenced by the composition of the minerals [5], the hydration heat obtained immediately
206 after the addition of water to the cement was not taken into consideration in the measurement. In this
207 test, the measurements were only carried out on samples prehydrated at 23, 43, 60, 85 and 98 RH for
208 180 days. The hydration heat of the sample prehydrated for 0 days was taken as a reference. The
209 measured heat flow and the cumulative heat were normalized to the clinker mass.

210

211 Finally, the hydration stopped CSA clinker powder that was prehydrated for 180 days was used to link
212 the **prehydration** effect with the clinker hydration products. The obtained powder was mixed with water
213 to have a water/binder ratio of 1. At the stage of **the** dormant period (2h), the main hydration period
214 (10h for PY sample and 12h for 7Y3A sample), and the final period (24h) of clinker hydration, the
215 hydrated clinker was subjected to hydration stoppage and ground. The mineral composition of the

216 hydrated clinker was characterized by XRD and TGA. The phase assemblage was analysed by QXRD
217 using an external standard.

218

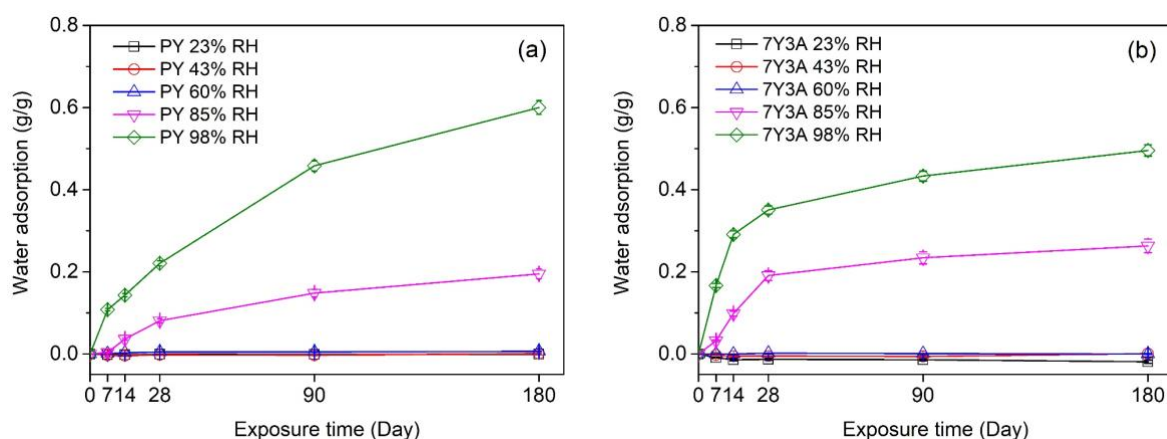
219 3. Result and discussion

220 3.1 Prehydration mechanism of CSA clinker

221 3.1.1 Water sorption kinetics

222 Fig. 2 shows results from the water adsorption test carried out on PY (a) and 7Y3A (b) samples exposed
223 to different RH. The weight increase of the clinker powder was recorded for a maximum of 180 days.

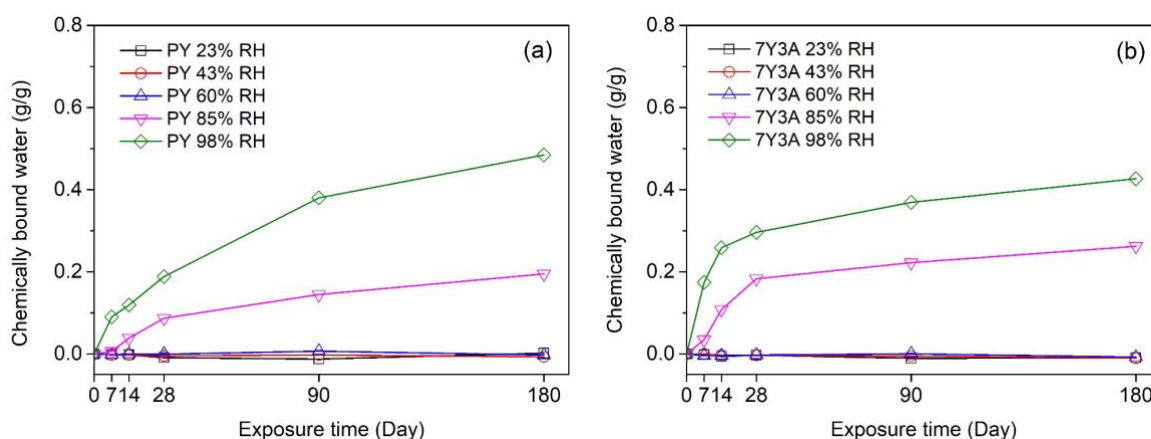
224 It is apparent that only clinker samples exposed to 85% and 98% RH show an increase of absorbed
225 water, irrespective of whether the anhydrite was added or not. **Contrary to the OPC cement in which**
226 **the free CaO in the clinker starts to hydrate at 55%RH [12]**, no water adsorption was found in CSA
227 clinker aged at 23, 43 and 60% RH; a slight desorption was even observed on 7Y3A sample exposed to
228 23% RH. For the PY sample aged at 98% RH, the **amount of** adsorbed water increased almost linearly
229 for the first 28 days, from 0 to about 0.22 g per gram of ignited clinker. Afterwards, it increased steadily
230 up to 0.6 g/g. When the ambient RH decreased from 98 to 85%, the water sorption kinetics decreased
231 correspondingly. Only 0.2 g/g water adsorption was found after 180 days of exposure. In case of
232 anhydrite blended with ye'elimitite clinker (7Y3A), the water adsorption was obviously different. The
233 water adsorption rate increased sharply for 7Y3A samples aged under 85 and 98% RH during the first
234 28 days. Afterwards, however, the exposure of 7Y3A clinker to 85 and 98% RH for additional 152 days
235 led to an increase of bound water of only about 0.03 and 0.06 g, respectively.



236 **Fig. 2** The amount of water held by (a) PY and (b) 7Y3A clinker exposed to water vapor of different RHs for a
237 maximum 180 days.

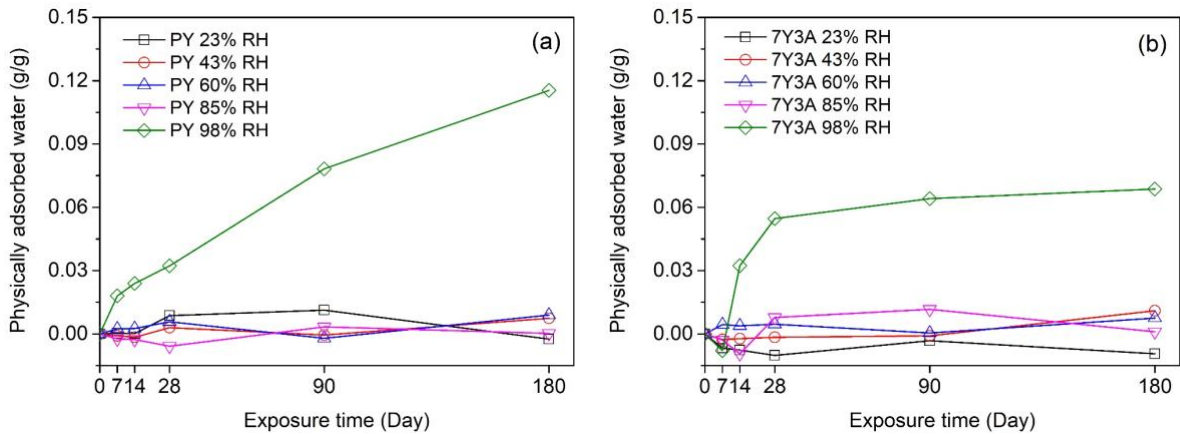
238 Although the results of water adsorption tests clearly suggest that the ambient water starts to be adsorbed
239 on the PY and 7Y3A clinker materials when the ambient RH is higher than 85%, it is unfortunately not
240 possible to differentiate between the water that is physically adsorbed on the surface of the clinker
241 powder and the water that is chemically bound in the inter-channel of the hydrates. To have a better
242 understanding of these differences at various conditions, the amount of chemically bound water was
243 calculated using Eq. 2, based on the TGA data. The results are shown in Fig. 3. In general, for both the

244 PY and the 7Y3A samples, the chemically bound water exhibits a very similar growth pattern as the
 245 overall result of water adsorption: only samples exposed to ambient RH higher than 85% showed an
 246 increase in the amount of chemically bound water. It is noteworthy that there is a 7-day induction period
 247 for the onset of chemical water adsorption, **observed for** both the PY and the 7Y3A samples exposed to
 248 85% RH. This may be caused by the exposure conditions - when a porous material is exposed to water
 249 vapour, an adsorption equilibrium is not established immediately due to the limited water activity. A
 250 similar phenomenon has been observed previously for tricalcium aluminate (C_3A): less than 1% degree
 251 of hydration of C_3A was achieved after the samples were exposed to 75% RH for 7 days whereas the
 252 degree of hydration surged up to 6% after 14 days [8]. A possible reason for the existence of this
 253 induction period can be the instability in exposure conditions. When the clinker is first placed in the
 254 drying jar, the target water vapour pressure cannot be established immediately. It takes time for the
 255 evaporation of water molecules from the saturated salt solution to reach an equilibrium vapour pressure
 256 in the sealed environment. Moreover, even if the vapour pressure reached an equilibrium in the drying
 257 jar, it is believed that the diffusion of water molecules from the ambient to the solid surface of the
 258 clinker, **which** finally results in the hydration of the clinker, will also delay the formation of chemically
 259 bound water. This assumption can be proven by the immediate growth of the chemically bond water
 260 when samples are exposed to an environment with higher RH (98%). Under high RH, the concentration
 261 of water molecules is much denser in the environment. There are more sites for the water molecules to
 262 react with the clinker. In that case, diffusion of water molecules from the environment to the clinker
 263 surface becomes easier.



264 **Fig. 3** The amount of chemically bound water held by (a) PY and (b) 7Y3A clinker exposed to water vapor of
 265 different RHs for a maximum 180 days.
 266

267 Finally, the amount of physically bound water was calculated by subtracting the weight of chemically
 268 bound water from the total sample weight after water adsorption (Fig. 4). It was found that only samples
 269 exposed to 98% RH show a significant increase **in the amount** of physically bound water. The PY
 270 clinker seems to have more **physically bound** water than the 7Y3A clinker. The reason for this difference
 271 is not clear. It may be due to the difference in porosity and **water adsorption** between ye'elinite and
 272 anhydrite.



273 **Fig. 4** The amount of physically bound water held by (a) PY and (b) 7Y3A clinker exposed to water vapor of
 274 different RHs for a maximum 180 days.

275

276 3.1.2 Degree of hydration

277 It has been proposed [30, 31] that the loss of chemically bound water of OPC can be defined as the
 278 weight loss between the weight after solvent exchange and the weight exposure to 550 °C. For CSA
 279 clinker, the main hydration products (ettringite, monosulfate and aluminum hydroxide) are believed to
 280 dehydrate above 50 °C at low RH [10], while no mass loss occurs after the clinker is heated up to 550 °C.
 281 Therefore, the weight loss between 50°C (after the solvent exchange) and 550°C can be attributed to
 282 the dehydration of chemically bound water. Based on the TGA results, the degree of hydration is
 283 calculated using Eq. 1, and the results are summarized in Table 4. As can be seen from the table, both
 284 the PY and the 7Y3A clinker remained unhydrated after exposure at 23%, 43% and 60% RH up to 180
 285 days. With the increase of RH from 60% to 85%, the onset of prehydration is observed. Both clinker
 286 minerals, PY and 7Y3A, show an increase of hydration degree during the prehydration exposure at 85%
 287 and 98% RH. However, the growth trend is different. The prehydration rate of ye'elimite blended with
 288 anhydrite (7Y3A) seems to be faster than prehydration of pure ye'elimite (PY) during the initial period
 289 of 28 days. The degree of hydration increased from 5.4% to 28.3% at 85% RH and from 27% to 45.8%
 290 at 98% RH for the 7Y3A sample. This is significantly higher than prehydration of the PY sample, in
 291 which the hydration degree increased from 1.1 to 15.6% and from 16 to 33.9% under the same
 292 conditions. The prehydration of ye'elimite is promoted by the addition of the sulfate phase. However,
 293 after the initial period of 28 days, the prehydration rate of the PY samples increased. This is more
 294 prominent for the PY sample exposed to 98% RH, as the degree of hydration of the PY sample at 90
 295 days is more than double than that at 28 days. The degree of hydration steadily increased further,
 296 reaching 87.3% at 180 days, which is 20% higher compared with 7Y3A sample. Overall, based on the
 297 degree of hydration, the safety threshold RH for CSA clinker storage can be identified as 60% RH.

298

299

Table 4 Degree of hydration of PY and 7Y3A clinker exposed to various RH.

	Time (Days)	Exposure RH (%)				
		23	43	60	85	98
7Y3A	7	0	0	0	5.4	27
	14	0	0	0	16.7	40
	28	0	0	0	28.3	45.8
	90	0	0	0	34.4	57.1
	180	0	0	0	40.6	66.1
PY	7	0	0	0	1.1	16
	14	0	0	0	6.9	21.5
	28	0	0	0	15.6	33.9
	90	0	0	0	26	68.4
	180	0	0	0	35	87.3

300

301 3.1.3 Assemblages of mineral phases

302 To further investigate the **prehydration** mechanism, XRD and TGA were used to characterize the
303 dynamic evolution of phase assemblages in the prehydrated clinker. As no significant differences of
304 phase assemblages were found among samples exposed to 23%, 43% and 60% RH, only the results of
305 PY and 7Y3A samples exposed to 60% RH are reported here. The term in the figure “Ref” refers to the
306 result of freshly sintered clinker powder. Figure 6 shows the results of XRD and TG analysis.

307

308 **60% RH**

309 From Fig. 5(a1) **it can be seen** that, compared with the Ref sample, no visible intensity changes or shifts
310 of XRD peaks can be observed from PY and 7Y3A samples. Ye’elimite is the dominant phase for the
311 PY sample with a trace of hard burnt anhydrite. When anhydrite was added into pure ye’elimite, the
312 characteristic peak of anhydrite could be clearly observed (Fig. 5 (b1)). This suggests that no new crystal
313 mineral has formed in PY and 7Y3A samples, even after 180 days exposure at 60% RH. TGA
314 measurements were performed to supplement the XRD analysis. It is clear that no significant mass loss
315 for both the PY (Fig. 5 (a2)) and the 7Y3A (Fig. 5 (b2)) samples can be detected from the TG
316 measurements when heating the clinker from 50 to 600°C, which indicates that no main hydration
317 products were formed during the **prehydration** exposure, neither in crystal nor in XRD-amorphous form.

318

319 **85% RH**

320 At **prehydration** condition of 85% RH, obvious changes of mineral assemblages can be observed from
321 the XRD patterns. For PY-85% RH sample, the formation of ettringite was identified after it was
322 exposed to 85% RH for 28 days, accompanied with decreased peak intensities of ye’elimite (Fig. 5(c1)).
323 Meanwhile, microcrystalline aluminium hydroxide (Gibbsite) occurs in an XRD broad peak form from

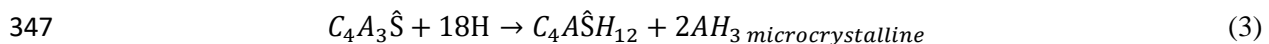
324 14 days. The characteristic peak of monosulfate (Ms) was hardly visible until the clinker was
325 prehydrated for 90 days, probably due to the poor crystallinity of monosulfate when it forms at air
326 exposure. Similar information can be obtained from the TGA analysis (Fig. 5 (c2)), from which
327 monosulfate with multiple broad characteristic peaks at around 70-150 and 150-200 °C can be identified.
328 Ettringite cannot be clearly distinguished from the DTG curve after the first 28 days, as it is only present
329 in minor amounts and its dehydration peak overlaps with the one of monosulfate. With the increase of
330 exposure time to 90 days, more intense peaks were observed at around 100-120 and 250-290°C,
331 representing the steady formation of ettringite and gibbsite, respectively. For the 7Y3A sample exposed
332 to 85% RH, when anhydrite is added to ye'elimite, ettringite occurs as the main hydration product of
333 the prehydrated clinker, accompanied with gibbsite (Fig. 5 (d1)). In the meantime, the amounts of
334 anhydrite and ye'elimite decreased correspondingly. This is further supported by the DTG curves,
335 where only peaks assigned to ettringite and gibbsite are present (Fig. 5 (d2)). A relatively weak
336 characteristic signal of microcrystalline aluminium hydroxide was detected via DTG compared to pure
337 ye'elimite clinker, which can be explained by the dilution of the ye'elimite with sulfate, leading to the
338 formation of less amorphous aluminate phase and more microcrystalline aluminium hydroxide in the
339 clinker. Similar findings have been previously reported [5].

340

341 **98% RH**

342 The **prehydration** behaviour of PY and 7Y3A samples at elevated RH of 98% is similar to that **observed**
343 at 85% RH, while the changes in mineral composition become more intense. As it was hydrated in
344 higher moisture condition, monosulfate and aluminium hydroxide formed in the PY sample with
345 depletion of ye'elimite according to Eq. 3 [3].

346



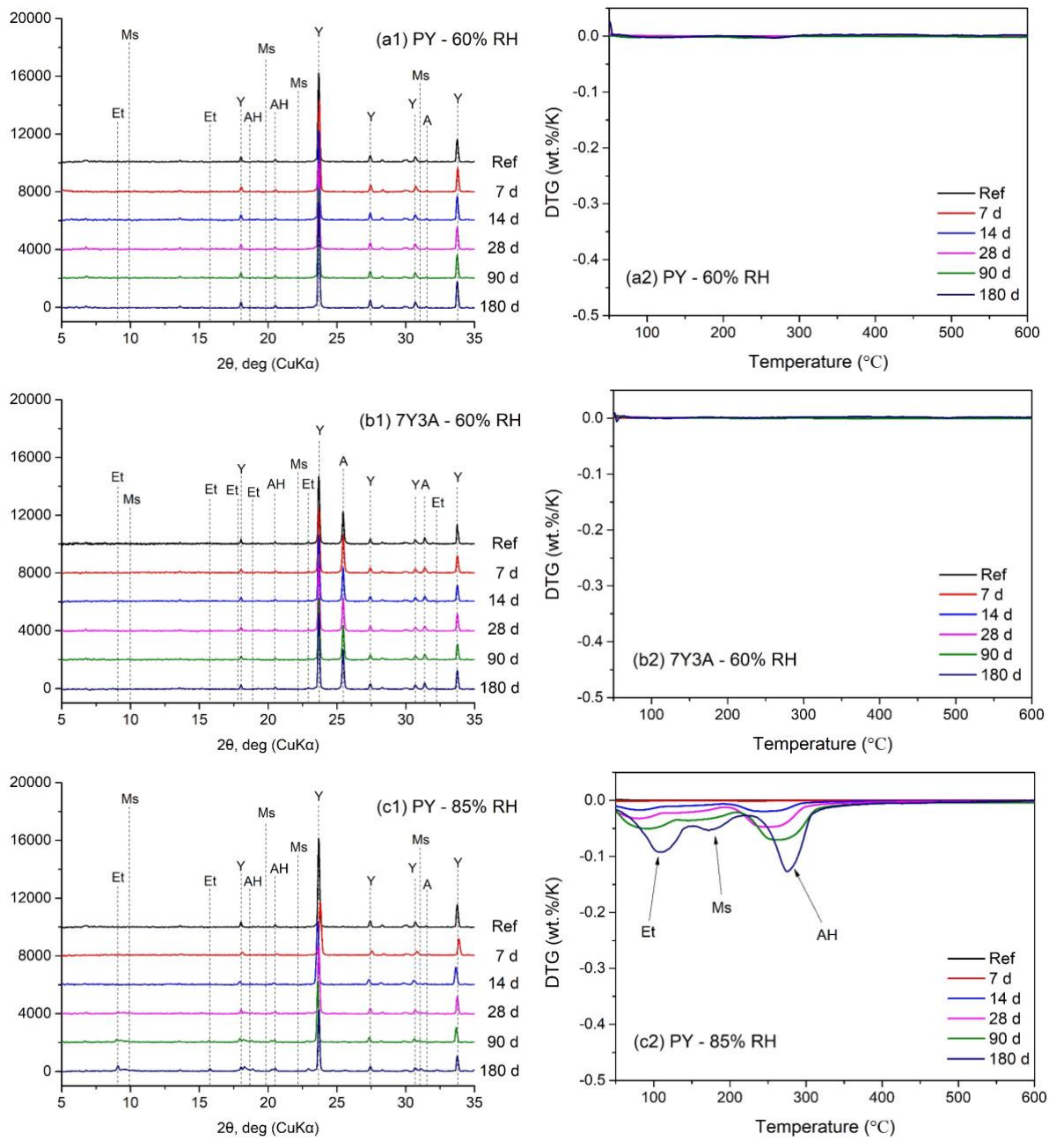
348

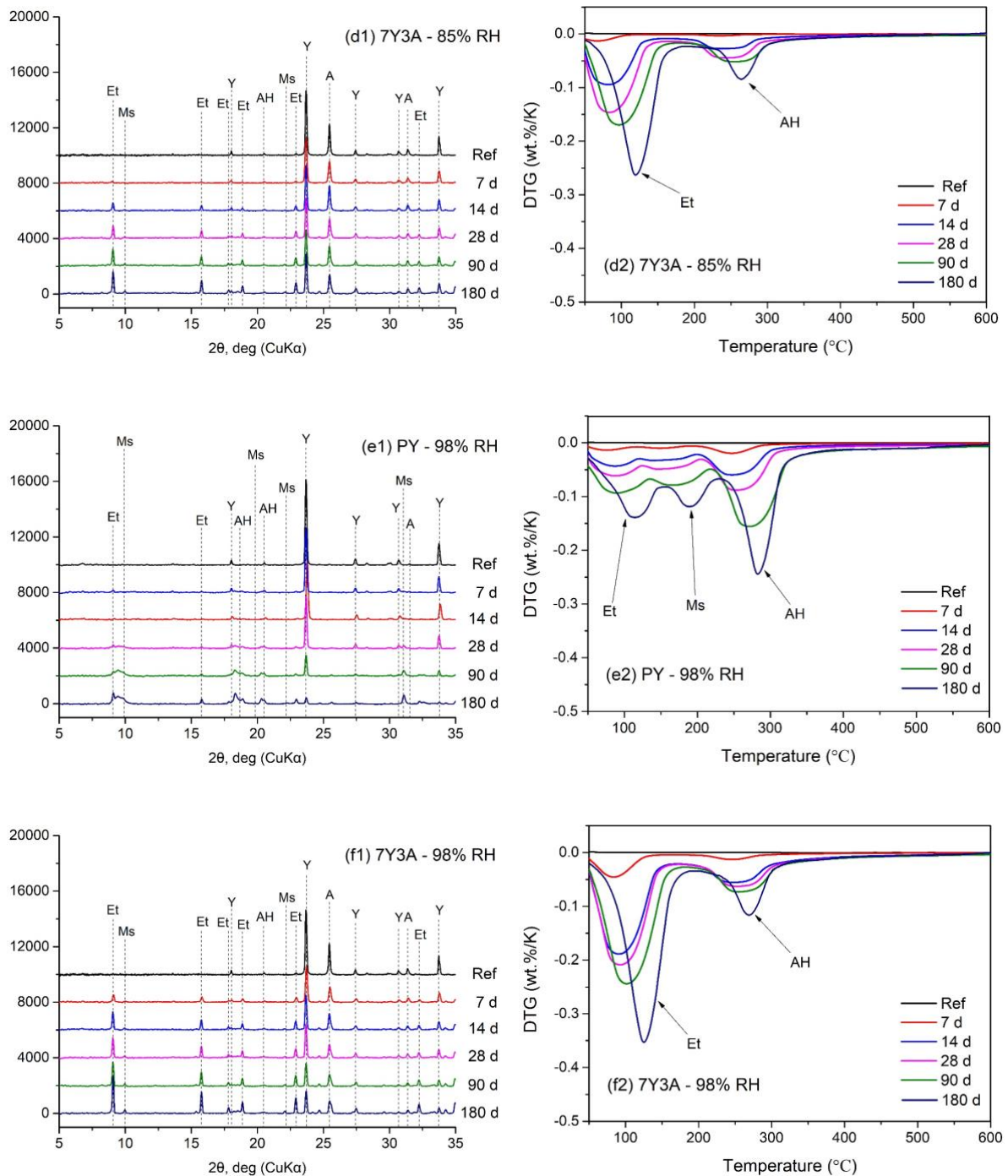
349 After exposure at 98% RH for 90 days, almost all ye'elimite presented in the PY sample has been
350 consumed and ettringite occurs as a minor hydration product (Fig. 5 (e1)). In the DTG diagram (Fig. 5
351 (e2)), aluminium hydroxide with the mass loss between 250 - 300°C appears to be the most predominant
352 **prehydration** product after long term exposure to higher RH, apart from monosulfate. The main
353 hydration product of 7Y3A that formed at 98% RH is recognized as ettringite, while traces of
354 monosulfate could also be identified after 90 days of exposure (Fig. 5 (f1)). Unlike the PY sample,
355 ye'elimite and anhydrite were not fully consumed even after being exposed to 98% RH for 180 days
356 since the pertinent characteristic peak can be observed clearly in the XRD pattern.

357

358 Moreover, a shift is observed in the characteristic peaks of DTG **with increased exposure duration**, from
359 lower dehydration temperature to higher dehydration temperature. Longer exposure leads to a higher

360 amount of chemically bound water. **Therefore**, this shift can be attributed to the dehydration of a larger
 361 amount of chemically bound water, resulting in higher vapour pressure in the environment of the solid,
 362 thus higher temperatures are needed to dehydrate the clinker. A similar phenomenon has been reported
 363 when a larger amount of gypsum was present in the sample [32].
 364



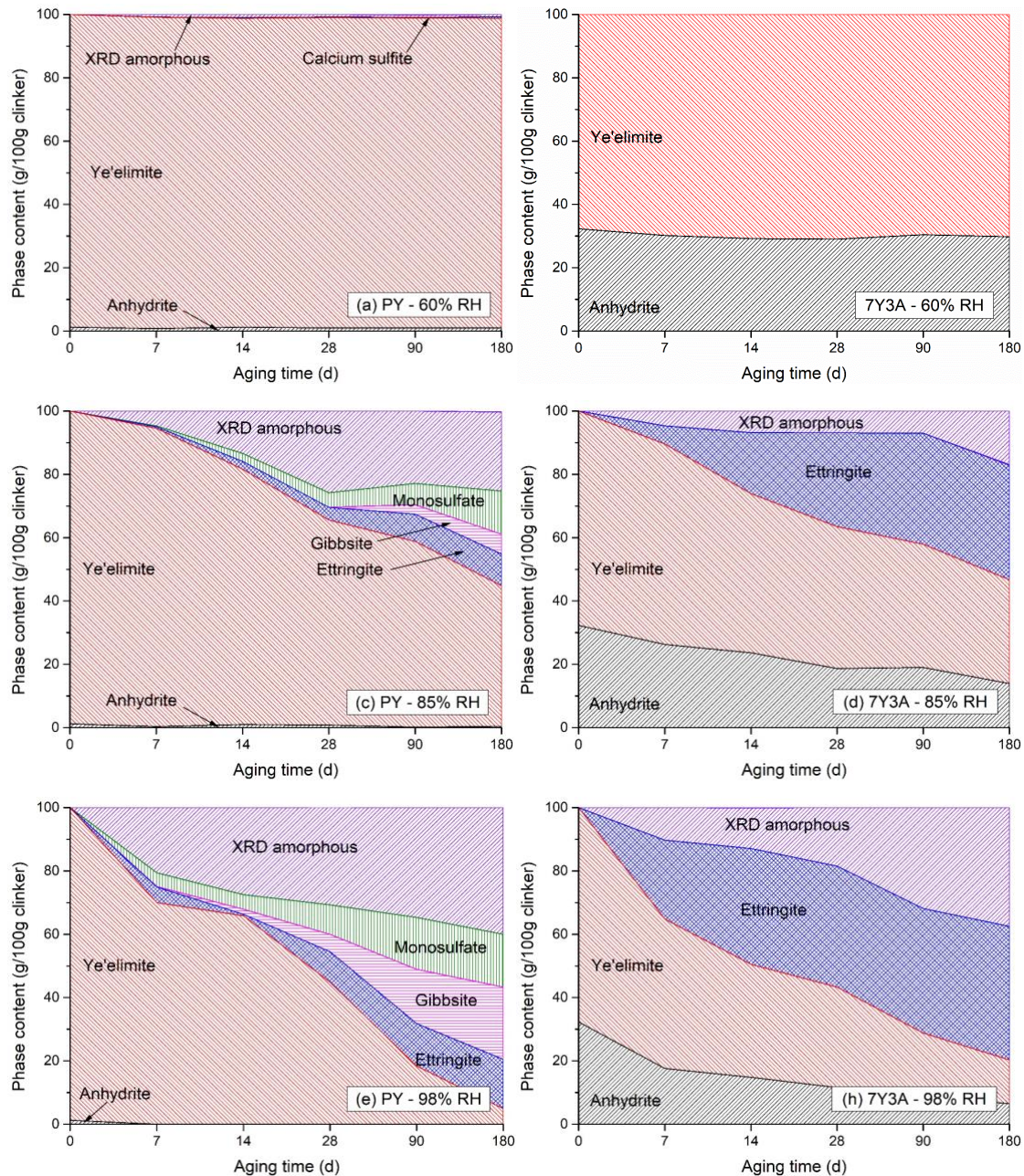


365 **Fig.5** Comparative study of XRD (left) and DTG (right) results of PY and 7Y3A clinker aged at (a, b) 60%, (c,
 366 d) 85% and (e, f) 98% RH for 0 (Ref), 7, 14, 28, 90 and 180 days.

367 3.1.4 QXRD analysis of phase assemblage

368 Since amorphous mineral phases such as aluminium hydroxide cannot be characterized from the XRD
 369 pattern, additional information of the phase assemblage of the prehydrated clinkers were obtained using
 370 Rietveld refinement coupled with an external standard method. The results are shown in Fig. 6.

371



372

373

374

375 **Fig.6** The dynamic of phase assemblage of PY (left) and 7Y3A (right) clinker exposed to (a, b) 60%, (c, d) 85%
 376 and (e, f) 98% RH for up to 180 days.

377 No obvious phases change was observed in neither the PY (Fig. 6a) and the 7Y3A (Fig. 6b) samples
 378 exposed to 60% RH after the 180 days of **prehydration**. However, despite the existence of the hard-
 379 burnt anhydrite originally coming from the sintered clinker, trace amounts (less than 0.5%) of XRD
 380 amorphous and calcium sulfite ($\text{CaSO}_3 \cdot (\text{H}_2\text{O})_{0.5}$) were found in the PY sample after 7 days of exposure
 381 at 60% RH. It has been reported that low RH favours formation of solid products with low water content
 382 [8]. The formation of these two phases with low water content can be attributed to the dissolution of
 383 ye'elimite and hard-burn anhydrite under low RH. With prolongation of the **prehydration** time from 7
 384 days to 180 days, the amount of XRD amorphous phases and calcium sulfite remained stable, without
 385 further increase.

386

387 When the storage humidity is increased to 85% RH, amorphous aluminium hydroxide (XRD amorphous)
388 is the first **prehydration** product formed in the PY clinker during the initial 7 days of **prehydration** (Fig.
389 6c). This is similar to the case previously reported for CSA initially hydrated in water [33], where
390 amorphous aluminium hydroxide, instead of monosulfate and microcrystalline aluminium hydroxide,
391 was considered to form as a result of dissolution of ye'elimite. With **longer prehydration** time, the
392 amount of ye'elimite decreases, which leads to the formation of ettringite and monosulfate, followed
393 by gibbsite at 28 days. Unlike the PY sample, no gibbsite and monosulfate were **observed** from the
394 XRD result for the 7Y3A sample even after 180 days of exposure (Fig. 6d). Ettringite, accompanied
395 with XRD-amorphous phases, is the main **prehydration** product due to the sufficient supply of sulfate.

396

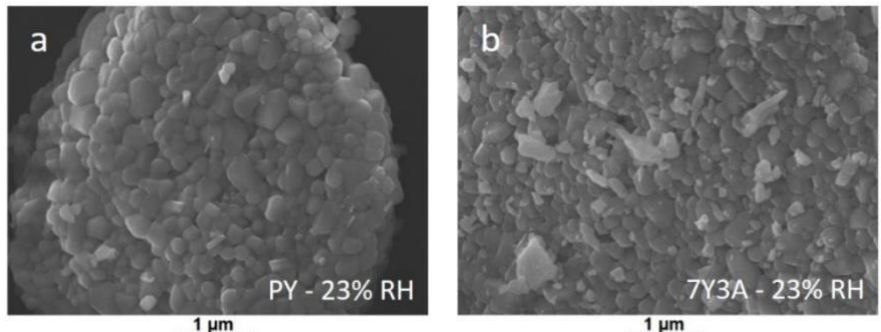
397 The tendency of both PY and 7Y3A samples at 98% RH is similar to that found at 85% RH. New phases
398 did not form with the increase of RH. Ye'elimite in the PY sample was almost depleted after 180 days
399 exposure at 98% RH (Fig. 6e). Moreover, it is interesting to note that the phase content of XRD
400 amorphous, monosulfate, gibbsite and ettringite of PY sample exposed to 85% RH for 180 days are
401 25%, 13.6%, 6.3% and 10% respectively, values which are almost equivalent to those of the PY sample
402 exposed to 98% for 28 days. The phase assemblages of the PY and the 7Y3A samples exposed to 85%
403 and 98% for 180 days are **in good** agreement with the literature [33].

404

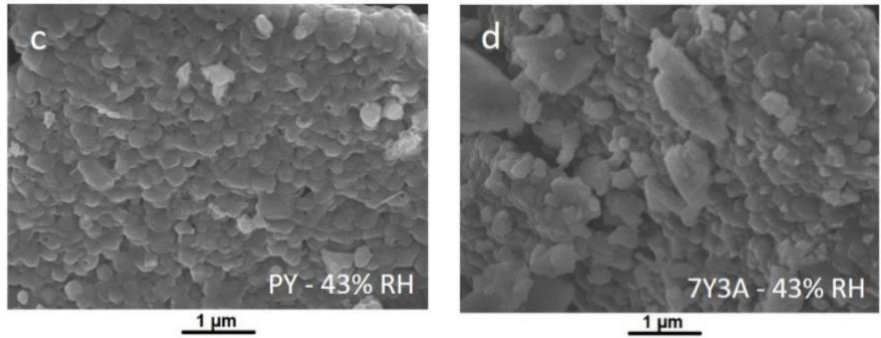
405 3.1.5 ESEM

406 ESEM was employed to study the morphology of ye'elimite dissolution and the precipitation of
407 hydration products. Fig. 7 shows SEM micrographs of clinkers prehydrated at different RH for 180
408 days. Similar to the results obtained from XRD and TGA, no obvious differences can be seen **between**
409 **the PY and the 7Y3A** samples exposed to 23% and 43% RH, and the Ref sample. Grains of anhydrous
410 particles are closely attached together, and no dissolution or precipitation occurs under this condition.
411 For **the PY** sample exposed to 60% RH, it is interesting to observe that globule-like particles have
412 formed on the surface of the clinker (Fig. 7e). **A similar** feature was described by Bullerjahn et. al. [34],
413 where the globule-like particles occurred when ye'elimite hydrated at 23 °C with a w/b ratio 100 for
414 420 seconds. The difference is that the globule-like particles **observed by Bullerjahn et al. [34]** are much
415 denser than **those observed** in the current study. This may result from the much more water molecules
416 **being** available when **the** clinker hydrates in liquid water compared to **being exposed to gaseous** water
417 vapour. According to the QXRD result in Fig. 6a, the globule-like particles observed on the PY - 60%
418 RH sample can be considered to be the trace amounts of XRD amorphous or calcium sulfite hydrates.
419 The formation of these globule-like particles can be regarded as onset of clinker hydration. From the
420 reaction kinetics point of view, **the** kinetic barrier of the hydration of clinker minerals is going to be
421 overcome at this water activity (RH). No globule-like particles **were observed in the 7Y3A** sample
422 (Fig.7f).

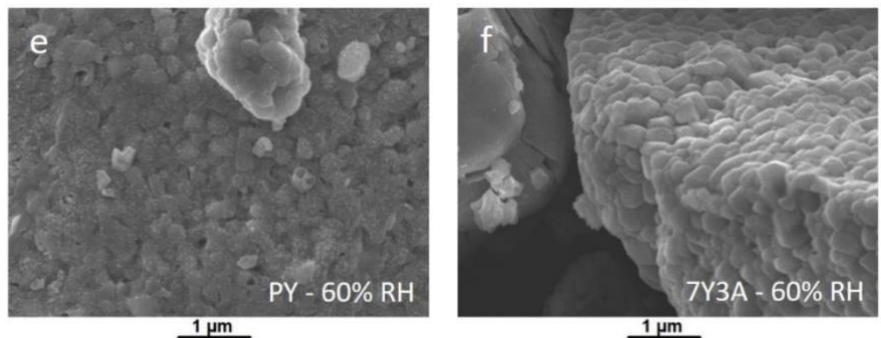
423



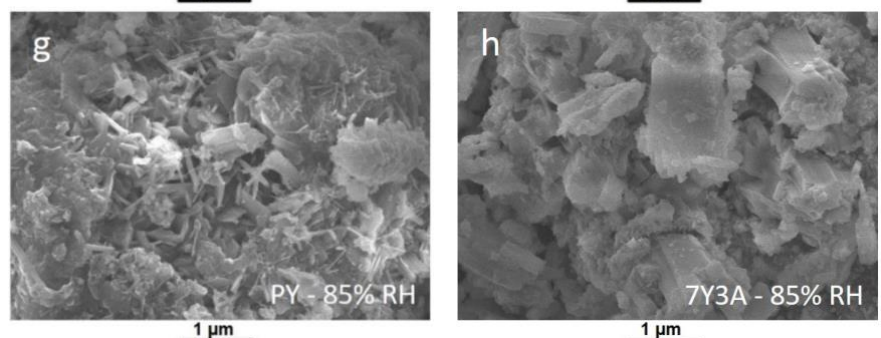
424



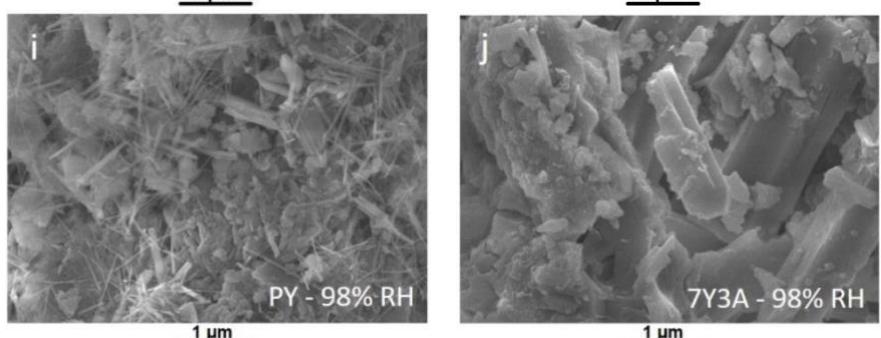
425



426



427



428

429

430

Fig.7 SEM images of PY (left) and 7Y3A (right) clinker exposed to (a, b) 23%, (c, d) 43%, (e, f) 60%, (g, h) 85% and (i, j) 98% RH for 180 days.

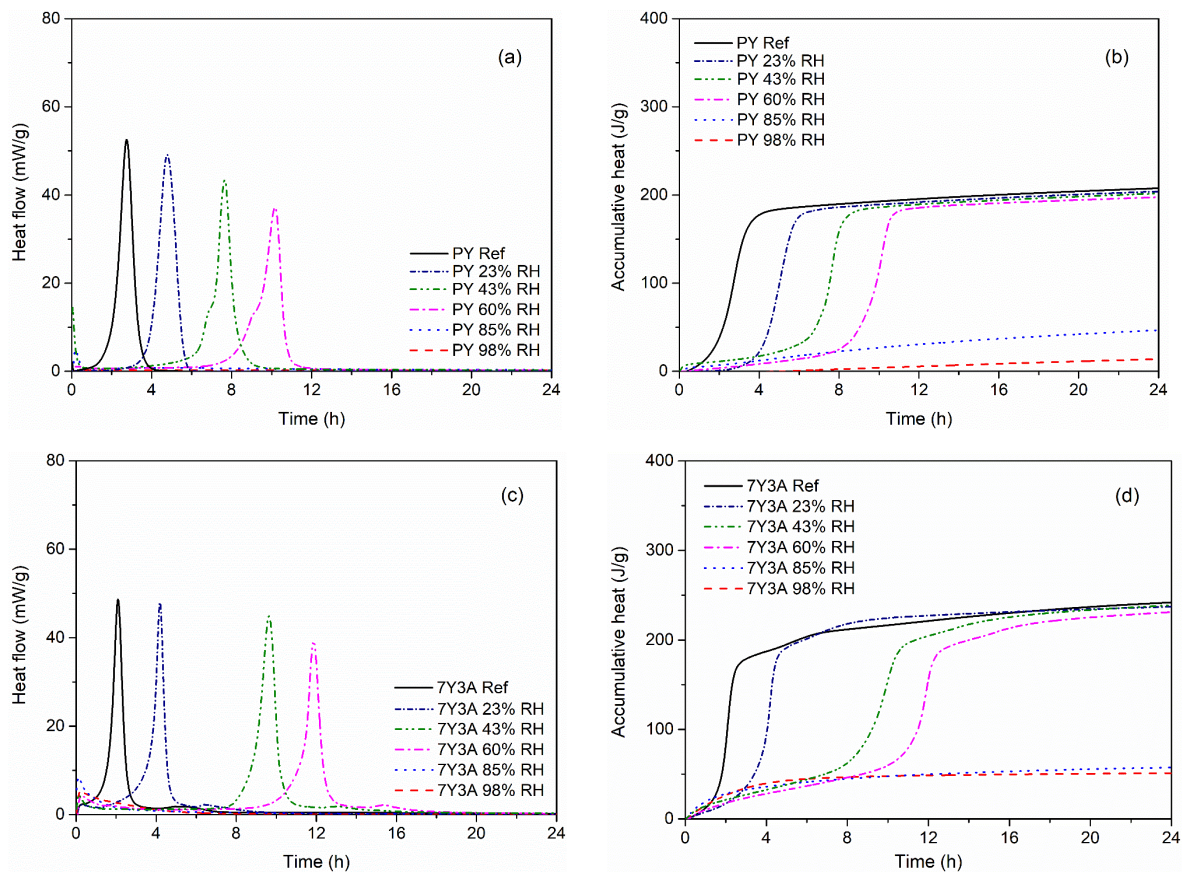
431 At 85% RH, prehydration causes obvious changes in the anhydrous CSA clinker morphology, while
 432 the hydration products of PY and 7Y3A seems to be different. For the PY sample (Fig. 7g), needle-like
 433 ettringite intermixed with amorphous or microcrystalline aluminium hydroxide has formed. Meanwhile,
 434 flake-like monosulfate can also be clearly identified. When anhydrite was added (Fig. 7h), the
 435 hexagonal ettringite crystals in the 7Y3A sample became more obvious and the volume of such needle-
 436 like crystals is much higher than that observed in the PY sample. No monosulfate can be observed in
 437 the images of the 7Y3A sample, which agrees well with the XRD analysis. With increase of RH from
 438 85% to 98% RH, more hydration products can be observed. Ettringite needles in the PY sample at 98%
 439 RH (Fig. 7i) seem longer than those observed at 85% RH. A lower amount of amorphous or
 440 microcrystalline aluminium hydroxide with more hexagonal ettringite crystals was found in the 7Y3A
 441 sample (Fig. 7j). It should be noted that the clinker powder has already coagulated and became a solid
 442 block after 28 days of exposure at 85% RH. Therefore, it can be considered unsuitable for practical
 443 applications.

444

445 3.2 Influence of clinker prehydration on the hydration products

446 3.2.1 Isothermal calorimetry

447 To further investigate the influence of prehydration humidity on the hydration of CSA clinker, 8-
 448 channel isothermal calorimetry was used to measure the hydration reactivity of the CSA clinker
 449 prehydrated at different RHs for 180 days. The results are shown in Fig. 8.



450 **Fig.8** Heat flow (left) and accumulate heat (right) of (a, b) PY and (c, d) 7Y3A clinker aged at different RHs for
451 180 days.

452

453 In general, for both the PY and the 7Y3A sample, the increase of prehydration humidity causes a
454 deceleration of the hydration activity, as shown by the delayed occurrence of the main hydration peak.
455 Compared with the Ref sample, a broader but a less intensive main hydration peak occurs with
456 increasing the prehydration humidity from 23 to 60% RH. This may be linked to the very slow process
457 of surface relaxation/reconstruction of clinker grains at ascending RH. A less active layer of dissolved
458 ye'elimite, which is difficult to observe in SEM micrographs, might have formed on the surface of
459 clinker grains. Some evidence for such an effect has been put forward for OPC systems by Dubina et
460 al. [35], who noted that C₃S hydration is retarded by extending the exposure duration of C₃S. The
461 formation of this passivation layer could slow down the migration of water molecules from the
462 environment to the interior of clinker grains and therefore delay the occurrence of main hydration peak.
463 With the increase of the storage relative humidity, the passivation layer became denser which could
464 result in delaying the occurrence of the main hydration peak of the PY sample from 2.7 h (PY-Ref) to
465 10.1 h (PY 60% RH). As for the 7Y3A sample, the calcium sulfate addition accelerated the hydration
466 of ye'elimite [5]. Compared with the PY Ref and the PY 23% RH sample, the hydration peak of 7Y3A
467 Ref and 7Y3A 23% RH occurred earlier: from 2.7 and 4.8 h to 2.1 and 4.1 h, respectively. A further
468 increase of ambient humidity from 23 to 60% RH significantly delayed the occurrence of the main
469 prehydration peak to 9.7 h (7Y3A 43% RH) and 11.9 h (7Y3A 60% RH). Although the main hydration
470 peak was clearly delayed, the cumulative heat for both PY and 7Y3A specimens is more or less the
471 same, showing that the overall reactivity was less affected by increasing RH until 60%. Similar values
472 (approximately 200 J/g clinker) have been reported elsewhere for fresh CSA cement [13].

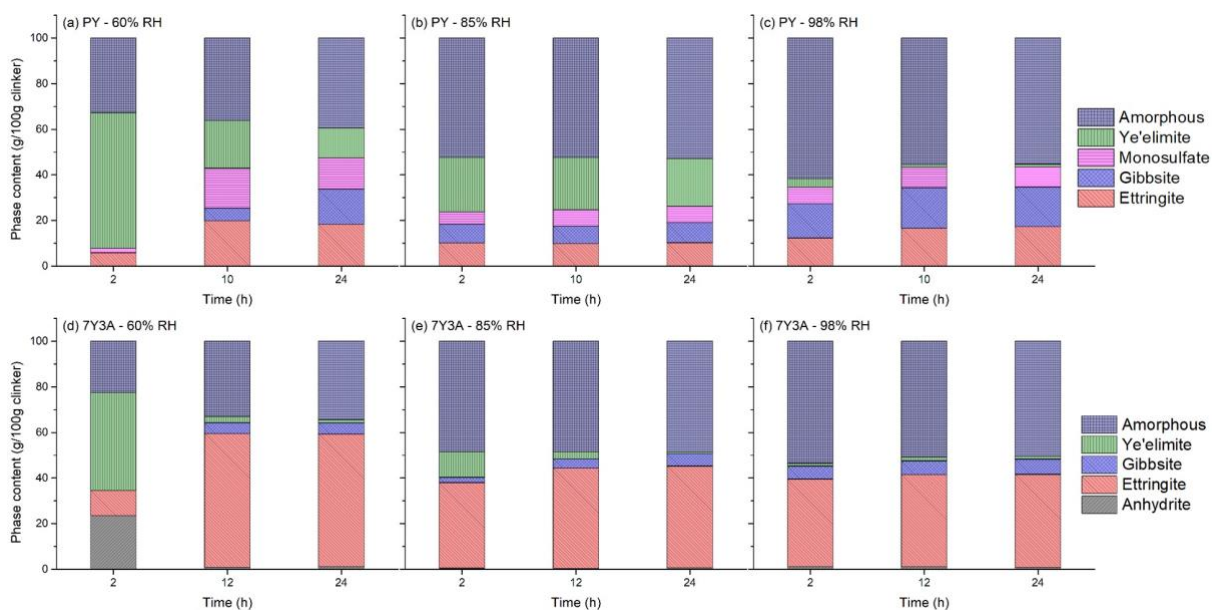
473 As soon as the ambient RH was increased to 85% RH, the balance between the dissolution of clinker
474 grains and the ambient humidity is broken and the passivation layer that covered the clinker grains
475 is penetrated by the larger number of water molecules. No significant hydration peak for neither the PY
476 nor the 7Y3A sample exposed to 85% and 98% RH could be detected in the later stage, and only a rapid
477 exothermic peak occurred directly when the sample is mixed with water. This peak can be attributed to
478 the heat of wetting and the very limited hydration reaction of ye'elimite clinker [5]. The PY sample
479 exposed to 98% RH showed the lowest cumulative hydration heat after 180 days of exposure, which is
480 consistent with the result of the degree of hydration and QXRD test as shown in table 1 and Fig. 6e,
481 respectively.

482

483 3.2.2 Hydration of CSA paste aged at various RH

484 In the previous section, it has been shown that the ambient humidity has a great influence on the mineral
485 composition of CSA clinker and the hydration of CSA cement paste [13]. However, the mineral
486 composition of the aged CSA clinker hydrated at different hydration stage is still not clear. In order to

487 have a deeper insight into the dynamic change of the mineral phase composition of hydrated CSA
 488 clinker, PY and 7Y3A sample aged at 60, 85 and 98% RH for 180 days were mixed with water with a
 489 water to cement ratio of 1:1. The mineral composition of aged CSA clinker hydrated during the dormant
 490 period (2h), the main hydration period (10h for PY sample and 12h for 7Y3A sample), and the final
 491 period (24h) was characterized by XRD and TGA, respectively, and the QXRD results are shown in
 492 Fig. 9. For PY and 7Y3A clinker exposed to 60% RH, a significant decrease of the anhydrous phase
 493 can be found with longer elapsed hydration time (from 2 to 24 h). Ettringite and amorphous phases are
 494 the two main hydration products **observed** after two hours of hydration. After that, a considerable
 495 proportion of gibbsite and monosulfate forms during hydration of the PY sample (Fig. 9a). On the other
 496 hand, for the 7Y3A sample, ettringite is the most predominant phase after 24 h of hydration, and
 497 accounts for almost 60% of the total (Fig. 9d). For the PY - 85%RH sample (Fig. 9b), the phase
 498 assemblage is constant throughout the 24 hours of hydration, which indicates that the hydration has
 499 finished. The amorphous phase is believed to originate from the **prehydration** process. In addition, a
 500 portion of unhydrated ye'elimite was still present in the hydrated clinker. It is not clear why ye'elimite
 501 has not hydrated, as no hydration heat could be detected by isothermal calorimetry after 12 hours of
 502 hydration (Fig. 8a). Only a slight change of phases was observed for the 7Y3A - 85%RH sample. A
 503 small portion of unhydrated ye'elimite was converted to ettringite and gibbsite (Fig.9e). Finally, for
 504 PY- 98%RH (Fig. 9c) and 7Y3A - 98%RH (Fig. 9f), no significant difference in phase assemblage was
 505 observed, despite that **the amount of XRD** amorphous phase was found to slightly decrease with longer
 506 hydration. This suggests that the hydraulic reactivity of CSA clinker has been almost **exhausted** by the
 507 **prehydration** process at 98% RH after 180 days. The decrease of amorphous phases can be attributed to
 508 the recrystallization of XRD-amorphous phases such as aluminate hydroxide.



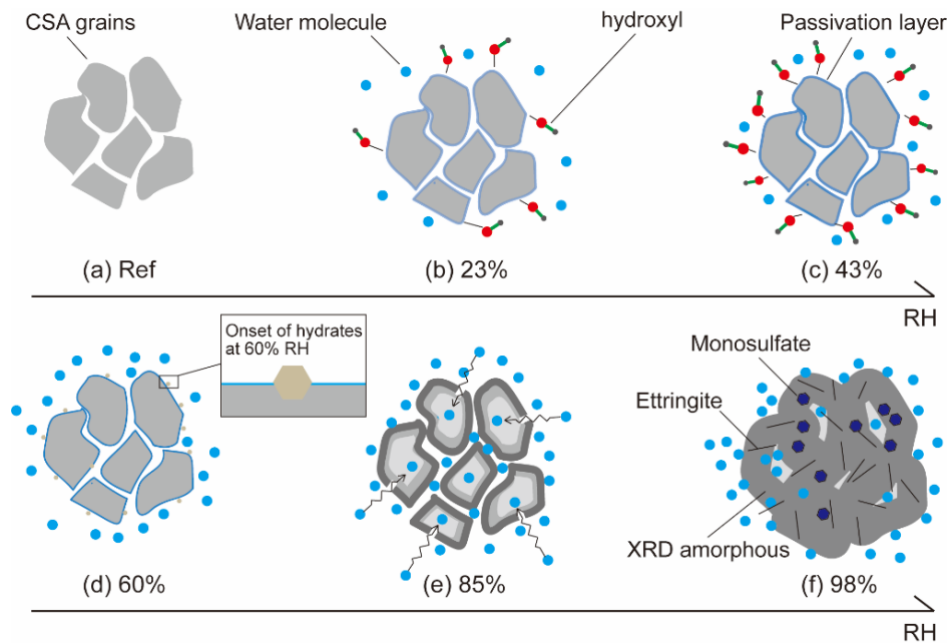
509

510 **Fig.9** Phase assemblage of **aged PY** clinker (a, b, c) and **aged 7Y3A** clinker (d, e, f) hydrated in water at
 511 different stages.

512

513 3.3 Mechanisms of RH affecting the hydraulic activity of CSA clinker

514 Based on the results presented above and the protective layer theory proposed by Dubina et al. on C_3S
515 and C_3A [35], the prehydration mechanism of CSA clinker composed mainly of ye'elimite can be
516 divided into two stages. A hypothesis for explaining the observed behavior is based on the passivation
517 layer theory, as schematically shown in in Fig. 10.



518

519 **Fig.10** Schematic diagram of prehydration mechanism of CSA clinker exposed to various RH.

520 The first stage is ranging from the freshly sinter clinker to clinker exposed to 43% RH (Fig. 10a - Fig.
521 10c). In this RH range, no sign of hydration was observed. Note that this does not mean that the
522 hydration of clinker will not happen at RH lower than 60%. However, a very long induction time must
523 precede this reaction. In a previous study, it was calculated that the induction time for C_3A can be 30000
524 years at 43% RH and 20°C [8]. With the increase of RH, more water molecules will be available in the
525 ambient air. According to the molecular diffusion theory, there is a higher chance of water molecules
526 to attack and be adsorbed on the clinker surface at high RH compared to lower RH. Theoretically, when
527 a porous material is exposed to water vapour, an equilibrium is not established immediately. Jensen [8]
528 calculated that the equilibrium between clinker and various mineral phases can only established at
529 extremely low RH (e.g., RH less than 1%). However, the fact is that no hydrates were found for neither
530 PY nor 7Y3A clinkers exposed to RH lower than 60%. A possible reason is that there ia very thin
531 passivation layer forms due to the adsorption and condensation of water molecules at the exposed surface
532 of clinker grains. Although the measuring techniques used cannot directly confirm this hypothesis, it
533 can be proven by the delayed occurrence of the exothermic peak of PY and 7Y3A after 180 days
534 exposure (see Fig. 8). As this passivation layer stops the water molecules from further penetrating into
535 the porous clinker, no further hydrates can form from the unhydrated clinker. Previously, Bullerjahn et
536 al. [5] attributed the long dormant period in the hydration heat of ye'elimite to a surface coverage of the

537 clinker grain by early hydration products. In an OPC system, the formation of this layer was termed
538 “surface hydroxylation” for tricalcium silicate hydrated in water at the very initial period [36]. It was
539 found in previous studies that the solubility of this passivation layer formed on the surface of tricalcium
540 silicate is 17 orders of magnitude lower than the one obtained from bulk thermodynamics [37, 38]. For
541 C₃A polymorphs, the formation of this liquid water film condenses on the surface of the phases was
542 regarded as a consequence of capillary condensation between the particles [39].

543 **Consequently**, 60% RH can be regarded as the threshold value for CSA clinker exposed to the ambient
544 humidity. At this turning point, although there are still no detectable hydrates formed, the onset of initial
545 hydrates such as globule-like XRD amorphous or calcium sulfite can be observed on the surface of CSA
546 clinker with the ESEM (Fig. 10 d). As the RH rises from 60% to 85%, the intensity of water molecular
547 diffusion increases further. The **prehydration** progress is significantly promoted by the increased water
548 activity. If the hypothesis that the existence of passivation layer is correct, the passive layer is supposed
549 to be pierced by the formation of initial hydrates. These spots where the initial hydrates form provide
550 pathways for the water molecules to get inside the porous clinker grains through capillary (Fig. 10 e).
551 Under this exposure, **prehydration** of clinker occurred as the hydration products such as ettringite and
552 monosulfate were observed after only 7 days of exposure at 85% RH. At 98% RH, the equilibrium of
553 the passivation layer between the clinker grain and the environmental water vapour pressure is broken
554 more rapidly. The hydration reaction starts immediately once the clinker is exposed to such water
555 vapour pressure. In that case, the CSA clinker is almost depleted after 180 days of exposure (Fig. 10 f).

556 **It should be pointed out that the current measurements performed in this study cannot directly confirm**
557 **and/or disprove the passivation layer theory described above. In fact, there is some controversy in the**
558 **literature related to whether the passivation layers can have an important effect on the water transport.**
559 **For example, Scrivener et al. [40] did not agree with the existence of any inhibiting layer formed by**
560 **dissolution and precipitation of a type of C-S-H on the surface. They suggested that dissolution**
561 **controlled by undersaturation is a better explanation for the induction period. Other authors do not**
562 **necessarily agree. For example, Galan and Andrade [40] showed, by direct observation, that passivation**
563 **layer of Portlandite does indeed occur when exposed to CO₂ at high RH. Therefore, further**
564 **investigations are needed to fully understand (and confirm or disprove) the mechanism. Advanced**
565 **instruments such as transmission electron microscopy (TEM) and X-ray photoelectron spectroscopy**
566 **(XPS) might be helpful in characterizing the formation of the passivation layer directly.**

567

568 **Conclusions**

569 In this investigation, the **prehydration** mechanism of CSA clinker stored under various RH conditions
570 has been experimentally studied. The hydration degree, phase assemblage, and hydration reactivity of
571 PY and 7Y3A samples after **prehydration** were characterized by means of TGA, XRD coupled with

572 Rietveld method, and isothermal calorimetry. The influence of anhydrite on the **prehydration** process
573 and products was investigated. The experiments revealed that:

574

- 575 1. Prehydration humidity plays an important role on the reactivity and usability of CSA cement. CSA
576 clinker must be stored in RH equal to or lower than 60% at atmospheric pressure. Exposure of
577 CSA clinker to RH above 85% will not only result in a significant decrease of hydraulic reactivity,
578 but also in agglomeration of clinker.
- 579 2. Similar to the clinker hydrated in water, the **prehydration** products of pure ye'elimite exposed to
580 RH at 85% or higher are ettringite, gibbsite, monosulfate and XRD amorphous, in which XRD-
581 amorphous is an important component at the initial period of **prehydration**. The addition of 30%
582 anhydrite results in significant changes to the hydration assemblage: only ettringite was found
583 formed besides XRD amorphous.
- 584 3. Although no apparent hydration products were found on **neither the PY** nor **the 7Y3A** sample
585 exposed to 60% RH, globule-like particles have formed on the surface of PY clinker, which can be
586 considered as a signal of the onset of prehydration.
- 587 4. Although increasing the RH from 23 to 60% RH has little effect on the clinker activity, a gradual
588 delay of the main hydration peak was observed with the increase of RH (from freshly sintered
589 clinker to clinker exposed to 60% RH). It is assumed that this is caused peak by the formation of
590 passivation layer.
- 591 5. After the clinker has been exposed to 85% and 98% RH for 180 days, hydraulic reactivity of both
592 PY and 7Y3A samples has almost been exhausted. The main hydration peak did no longer exist
593 when the aged CSA clinker was hydrated in water. Only slight changes in **the** phase assemblage
594 **were observed**.

595

596 **Acknowledgements**

597 The authors would like to acknowledge the financial support provided by the National Natural Science
598 Foundation of China (No. 51908368) and Natural Science Foundation of Guangdong Province (No.
599 2020A1515010939). The authors also would like to acknowledge the support from Guangdong
600 Provincial Key Laboratory of Durability for Marine Civil Engineering (No. 2020B1212060074).

601

602 **Reference**

- 603 [1] R.M. Andrew, Global CO₂ emissions from cement production, *Earth Syst. Sci. Data*, 10 (2018) 195-
604 217.
- 605 [2] C. Le Quéré et al., Global Carbon Budget 2017, *Earth Syst. Sci. Data*, 10 (2018) 405-448.
- 606 [3] L. Zhang, M. Su, Y. Wang, Development of the use of sulfo- and ferroaluminate cements in China,
607 *Advances in Cement Research*, 11 (1999) 15-21.
- 608 [4] E. Gartner, Industrially interesting approaches to “low-CO₂” cements, *Cement and Concrete*
609 *Research*, 34 (2004) 1489-1498.

610 [5] F. Winnefeld, S. Barlag, Calorimetric and thermogravimetric study on the influence of calcium
611 sulfate on the hydration of ye'elimite, *Journal of Thermal Analysis and Calorimetry*, 101 (2010) 949-
612 957.

613 [6] F. Winnefeld, B. Lothenbach, Hydration of calcium sulfoaluminate cements - Experimental findings
614 and thermodynamic modelling, *Cement and Concrete Research*, 40 (2010) 1239-1247.

615 [7] F.P. Glasser, L. Zhang, High-performance cement matrices based on calcium sulfoaluminate–belite
616 compositions, *Cement and Concrete Research*, 31 (2001) 1881-1886.

617 [8] O.M. Jensen, P.F. Hansen, E.E. Lachowski, F.P. Glasser, Clinker mineral hydration at reduced
618 relative humidities, *Cement and Concrete Research*, 29 (1999) 1505-1512.

619 [9] L.G. Baquerizo, T. Matschei, K.L. Scrivener, M. Saeidpour, A. Thorell, L. Wadsö, Methods to
620 determine hydration states of minerals and cement hydrates, *Cement and Concrete Research*, 65 (2014)
621 85-95.

622 [10] L.G. Baquerizo, T. Matschei, K.L. Scrivener, Impact of water activity on the stability of ettringite,
623 *Cement and Concrete Research*, 79 (2016) 31-44.

624 [11] C. Maltese, C. Pistolesi, A. Bravo, F. Cella, T. Cerulli, D. Salvioni, A case history: Effect of
625 moisture on the setting behaviour of a Portland cement reacting with an alkali-free accelerator, *Cement
626 and Concrete Research*, 37 (2007) 856-865.

627 [12] J. Stoian, T. Oey, J.W. Bullard, J. Huang, A. Kumar, M. Balonis, J. Terrill, N. Neithalath, G. Sant,
628 New insights into the prehydration of cement and its mitigation, *Cement and Concrete Research*, 70
629 (2015) 94-103.

630 [13] S. Ramanathan, B. Halee, P. Suraneni, Effect of calcium sulfoaluminate cement prehydration on
631 hydration and strength gain of calcium sulfoaluminate cement-ordinary portland cement mixtures,
632 *Cement and Concrete Composites*, 112 (2020) 103694.

633 [14] E. Dubina, L. Black, R. Sieber, J. Plank, Interaction of water vapour with anhydrous cement
634 minerals, *Advances in Applied Ceramics*, 109 (2010) 260-268.

635 [15] R.J. Flatt, G.W. Scherer, J.W. Bullard, Why alite stops hydrating below 80% relative humidity,
636 *Cement and Concrete Research*, 41 (2011) 987-992.

637 [16] F. Bullerjahn, J. Skocek, M. Ben Haha, K. Scrivener, Chemical shrinkage of ye'elimite with and
638 without gypsum addition, *Construction and Building Materials*, 200 (2019) 770-780.

639 [17] D. Jansen, A. Spies, J. Neubauer, D. Ectors, F. Goetz-Neunhoeffler, Studies on the early hydration
640 of two modifications of ye'elimite with gypsum, *Cement and Concrete Research*, 91 (2017) 106-116.

641 [18] R. Snellings et al., RILEM TC-238 SCM recommendation on hydration stoppage by solvent
642 exchange for the study of hydrate assemblages, *Materials and Structures*, 51 (2018) 172.

643 [19] P. Zhang, L. Shi, Y. Chen, Y. Zhang, W. Huang, X. Zhou, J. Wu, Preparation of pure mineral
644 C₄A₃Ŝ for sturcture analysis by orthogonal design, *Journal of China Building Materials Academy*, 1
645 (1989) 298-303.

646 [20] ASTM E104-02 "Standard Practice for Maintaining Constant Relative Humidity by Means of
647 Aqueous Solutions", ASTM International, West Conshohocken, PA, 2002.

648 [21] L. Greenspan, Humidity fixed points of binary saturated aqueous solutions, *Journal of Research of
649 the National Bureau of Standards Section A: Physics and Chemistry*, (1977) 89-96.

650 [22] J. Zhang, G.W. Scherer, Comparison of methods for arresting hydration of cement, *Cement and
651 Concrete Research*, 41 (2011) 1024-1036.

652 [23] M. Zajac, J. Skocek, C. Stabler, F. Bullerjahn, M.B. Haha, Hydration and performance evolution
653 of belite–ye'elimite–ferrite cement, *Adv Cem Res*, 31 (2019) 124-137.

654 [24] A. Cuesta, A.G. De la Torre, E.R. Losilla, V.K. Peterson, P. Rejmak, A. Ayuela, C. Frontera,
655 M.A.G. Aranda, Structure, Atomistic Simulations, and Phase Transition of Stoichiometric Yeelimite,
656 *Chemistry of Materials*, 25 (2013) 1680-1687.

657 [25] A. Kirfel, G. Will, Charge density in anhydrite, CaSO₄, from X-ray and neutron diffraction
658 measurements, *Acta Crystallographica Section B*, 36 (1980) 2881-2890.

659 [26] F. Goetz-Neunhoeffler, J. Neubauer, Refined ettringite (Ca₆Al₂(SO₄)₃(OH)₁₂·26H₂O structure for
660 quantitative X-ray diffraction analysis, *Powder Diffraction*, 21 (2006) 4-11.

661 [27] R. Allmann, Refinement of the hybrid layer structure hexahydroxoaluminocalcium
662 hemisulfate trihydrate (Ca₂Al (OH)₆)(1/2SO₄·3H₂O), *Neues Jahrbuch fur Mineralogie, Monatshefte*,
663 (1977) 136-144.

- 664 [28] H. Saalfeld, M. Wedde, Refinement of the crystal structure of gibbsite, $\text{Al}(\text{OH})_3$, Zeitschrift für
665 Kristallographie - Crystalline Materials, 139 (1974) 129.
- 666 [29] L. Schröpfer, Strukturelle Untersuchungen am $\text{CaSO}_3 \cdot 1/2\text{H}_2\text{O}$, Zeitschrift für anorganische und
667 allgemeine Chemie, 401 (1973) 1-14.
- 668 [30] A. Schöler, B. Lothenbach, F. Winnefeld, M. Zajac, Hydration of quaternary Portland cement
669 blends containing blast-furnace slag, siliceous fly ash and limestone powder, Cement and Concrete
670 Composites, 55 (2015) 374-382.
- 671 [31] K. De Weerd, M.B. Haha, G. Le Saout, K.O. Kjellsen, H. Justnes, B. Lothenbach, Hydration
672 mechanisms of ternary Portland cements containing limestone powder and fly ash, Cement and
673 Concrete Research, 41 (2011) 279-291.
- 674 [32] K. Scrivener, R. Snellings, B. Lothenbach, A practical guide to microstructural analysis of
675 cementitious materials, Crc Press 2018.
- 676 [33] W. Frank, L. Barbara, Phase equilibria in the system $\text{Ca}_4\text{Al}_6\text{O}_{12}\text{SO}_4\text{-Ca}_2\text{SiO}_4\text{-CaSO}_4\text{-H}_2\text{O}$ referring
677 to the hydration of calcium sulfoaluminate cements, RILEM Technical Letters, 1 (2016).
- 678 [34] F. Bullerjahn, E. Boehm-Courjault, M. Zajac, M. Ben Haha, K. Scrivener, Hydration reactions and
679 stages of clinker composed mainly of stoichiometric ye'elimite, Cement and Concrete Research, 116
680 (2019) 120-133.
- 681 [35] E. Dubina, R. Sieber, J. Plank, L. Black, Effects of pre-hydration on hydraulic properties on
682 Portland cement and synthetic clinker phases, 2008.
- 683 [36] P. Barret, D. Ménétrier, D. Bertrandie, Mechanism of C_3S dissolution and problem of the
684 congruency in the very initial period and later on, Cement and Concrete Research, 13 (1983) 728-738.
- 685 [37] H.M. Jennings, P.L. Pratt, An experimental argument for the existence of a protective membrane
686 surrounding portland cement during the induction period, Cement and Concrete Research, 9 (1979)
687 501-506.
- 688 [38] H.N. Stein, Thermodynamic considerations on the hydration mechanisms of Ca_3SiO_5 and $\text{Ca}_3\text{Al}_2\text{O}_6$,
689 Cement and Concrete Research, 2 (1972) 167-177.
- 690 [39] E. Dubina, J. Plank, L. Black, L. Wadsö, Impact of environmental moisture on C_3A polymorphs in
691 the absence and presence of $\text{CaSO}_4 \cdot 0.5 \text{H}_2\text{O}$, Adv Cem Res, 26 (2014) 29-40.
- 692 [40] K. Scrivener, A. Ouzia, P. Juilland, A. Kunhi Mohamed, Advances in understanding cement
693 hydration mechanisms, Cement and Concrete Research, 124 (2019) 105823.